Revista Ciência Agronômica, v. 54, e20217886, 2023
Centro de Ciências Agrárias - Universidade Federal do Ceará, Fortaleza, CE
www.ccarevista.ufc.br

*Scientific Article*
ISSN 1806-6690

# Development of a portable multisensor platform for soil mapping[1]

## Desenvolvimento de uma plataforma multisensor portátil para mapeamento de solo

**Emanoel Di Tarso dos Santos Sousa[2]*, Daniel Marçal de Queiroz[3], André Luiz de Freitas Coelho[3], Domingos Sárvio Magalhães Valente[3]**

**ABSTRACT -** Soil sensors are alternatively used to reduce the costs of soil sampling and be able to perform analyses in a laboratory. However, using individual sensors can result in low accuracy because the measured variable may be related to more than one soil characteristics. This study aimed to develop a portable soil multisensor platform with sensors for apparent electrical conductivity, moisture, temperature, and penetration resistance of the soil. The multisensor platform was developed based on a BeagleBone Black (BBB) single-board computer. Electronic circuits have been developed for electrical conductivity and moisture sensors. A load cell was used in the soil-penetration resistance sensor. For validation, the ECa, soil moisture, and penetration resistance data obtained using the multisensor platform and commercial sensors were compared. A low-cost global navigation satellite system module was used to georeference sampling points. The cost of acquiring the components required to assemble the multisensor platform was US$ 361.94. The strong correlation between the data obtained with the multisensor platform and commercial sensors proves that the developed multisensor platform has acceptable accuracy. The spatial variability of the apparent soil electrical conductivity, moisture, temperature, and penetration resistance in a coffee plantation can be characterized by the generated maps from the data obtained by the four sensors.

**Key words**: Apparent electrical conductivity. Soil penetration resistance. BeagleBone Black. Single-board computer. Soil sensors.

**RESUMO** - O uso de sensores de solo tem sido uma alternativa para a redução dos custos com amostragem e análise de solo em laboratório, permitindo a adoção de uma maior densidade amostral. O presente estudo teve como objetivo desenvolver uma plataforma multisensor portátil para solo, com sensores de condutividade elétrica aparente, umidade, temperatura e resistência do solo à penetração. A plataforma multisensor foi desenvolvida com base no computador de placa única BeagleBone Black (BBB). Para os sensores de condutividade elétrica aparente e sensor de umidade, circuitos eletrônicos foram desenvolvidos. Uma célula de carga foi utilizada no sensor de resistência do solo à penetração. Para validação, dados de ECa, umidade e resistência à penetração obtidos utilizando a plataforma multisensor e sensores comerciais foram comparados entre si. Um módulo GNSS (Global Navigation Satellite System) de baixo custo foi utilizado para georreferenciamento dos pontos de coleta de dados. O custo com aquisição dos componentes necessários para montagem da plataforma multisensor foi de US$ 361,94. Para ECa, umidade e resistência à penetração média e máxima a correlação entre os dados obtidos com a plataforma multisensor e com os sensores comerciais foram 0,95; 0,92; 0,90 e 0,91, respectivamente. A forte correlação comprova que a plataforma multisensor desenvolvida tem precisão aceitável. Os mapas gerados com os dados obtidos pelos quatro sensores permitiram caracterizar a variabilidade espacial da condutividade elétrica aparente, umidade, temperatura e resistência do solo à penetração em uma lavoura de café.

***Palavras-chave***: Condutividade elétrica aparente. Resistência do solo à penetração. BeagleBone Black. Computador de placa única. Sensores de solo.

DOI: 10.5935/1806-6690.20230008
Editor-in-Article: Prof. Fernando Bezerra Lopes - lopesfb@ufc.br
*Author for correspondence
Received for publication on 18/02/2021; approved on 15/09/2021
[1]Part of the first author's thesis, presented to Postgraduate Program in Agricultural Engineering, Universidade Federal de Viçosa, Viçosa, Minas Gerais. This study was funded by Coordination for the Improvement of Higher Education Personnel (CAPES, Brazil) and National Counsel of Technological and Scientific Development (CNPq)
[2]Departamento de Engenharia Agrícola, Universidade Federal Rural de Pernambuco (UFRPE), Recife-PE, Brazil, emanoel.sousa@ufrpe.br (ORCID ID 0000-0002-8290-899X)
[3]Departamento de Engenharia Agrícola, Universidade Federal de Viçosa (UFV), Viçosa-MG, Brazil, queiroz@ufv.br (ORCID ID 0000-0003-0987-3855), andre.coelho@ufv.br (ORCID ID 0000-0002-7595-9713), valente@ufv.br (ORCID ID 0000-0001-7248-8613)

## INTRODUCTION

In agriculture, the conventional technique of soil characterization in agriculture involves sampling and then physical and chemical analyses in the laboratory. However, as this technique is costly and time-consuming, farmers are forced to use low-density sampling points. Consequently, the generated maps of soil attributes may not represent the true spatial variability in the study area (MAHMOOD; HOOGMOED; VAN HENTEN, 2012). Therefore, proximal soil sensing technologies have been adopted. Some existing soil sensors measure the soil's pH, apparent electrical conductivity, moisture, penetration resistance, and spectral signature (ADAMCHUK *et al*., 2004).

Sensors are used as tools for soils' spatial characterization and hence are efficient and economical (MEDEIROS *et al*., 2016; STADLER *et al*., 2015). However, using a single sensor may lead to poor characterization of soil spatial variability because the variables determined by the sensor may be related to two or more soil attributes (MAHMOOD; HOOGMOED; VAN HENTEN, 2012). Conversely, using multiple sensors tends to provide a better characterization of soil spatial variability, reducing the decision-making errors due to a lack of accurate information (CHO *et al*., 2016).

Several studies have been conducted to develop and test sensing systems that can measure multiple soil variables (FISHER; KEBEDE, 2010; NADERI-BOLDAJI *et al*., 2019; YURUI *et al*., 2008). One option for the development of low-cost systems is using open-source software and hardware (COELHO *et al*., 2020), such as the BeagleBone Black (BBB, BeagleBone Rev. C) single-board computer, which is a compact platform with high processing speed, low power consumption, and low cost (MOLLOY, 2014).

This study aimed to develop a portable soil multisensor platform. The multisensor platform comprises sensors for apparent electrical conductivity, moisture, temperature, and penetration resistance. Low-cost components and open-source programming languages were used to reduce the device cost. Owing to the use of a portable multi-sensor platform, the cost was reduced, and areas inaccessible by wheeled vehicles could be mapped. A low-cost portable system is suitable for mapping soil in small areas. Therefore, smallholder farmers can adopt precision farming techniques.

## MATERIAL AND METHODS

### Components

A portable multisensor platform was developed with a BBB single-board computer as the main component. The BBB acquires signals from sensors and processes and stores data. The components connected to the BBB were a soil apparent electrical conductivity (ECa) sensor, soil moisture sensor, soil temperature sensor, soil penetration resistance sensor, global navigation satellite system (GNSS) module (Adafruit Technologies, New York), and a 178-mm touchscreen LCD (4D Systems, Australia). A 5-V 12-Ah portable battery was used as the power source for the multisensor platform (Figure 1). The battery, BBB, LCD screen, GNSS module, and electronic circuit of the sensors were installed in a box composing the central unit of the multisensor platform.

The soil ECa sensor was developed based on the electrical resistivity principle. Electrodes with the diameter and length of 6 and 60 mm, respectively, were used and were arranged according to the Wenner matrix. They were fixed on an aluminum rod at a 0.3-m spacing. This sensor has three circuits: a converter and amplifier circuit (CAC), potential difference measurement circuit (PDC), and signal conditioning circuit (SCC). The CAC amplifies and converts (from unipolar to bipolar) the signal generated by the pulse-width modulation port of the BBB. The converted and amplified signals were applied to the soil using current electrodes. The PDC was used to measure the potential difference in the internal electrodes and in a 180-Ω resistor. The first result refers to the difference in the potential generated by applying the signal to soil. The second result was used to determine the applied electrical current based on Ohm's law. The SCC was used to condition the potential difference signals generated by the PDC. Conditioning was necessary because the BBB can only read analog signals within the range of 0–1.8 V. Queiroz *et al*. (2016) and Queiroz *et al*. (2017, 2020) presented the detailed development of this sensor.

The soil moisture sensor was developed based on the astable operation mode of a 555 timer integrated circuit (IC), adapting the circuit proposed by Texas Instruments (2014). In the adapted circuit, the soil capacitance and 1 kΩ resistor form a resistive-capacitive low-pass filter, attenuating the voltage of the signal generated by IC 555 (Figure 2). Thus, soils with higher moisture values result achieve greater capacitance and, consequently, lower voltages of the output signal. The output signal was read using BBB analog ports. Two steel electrodes (diameter and length of 6 and 120 mm, respectively) were used to measure the soil capacitance. The electrodes were fixed onto an aluminum structure with a 30-mm spacing.

The moisture sensor was calibrated to determine the moisture content in the dry base and was used to measure moisture at sites with different soil moisture contents. During each reading, the voltage was recorded, and soil samples were collected. In the laboratory, the gravimetric moisture (in the dry base) of the samples was determined using the procedure

presented by Teixeira *et al*. (2017). The coefficients of the model that described moisture (in % dry base) are determined through polynomial regression as a function of the voltage generated by the circuit (Figure 3).

**Figure 1** - Scheme of the soil multisensor platform with the BeagleBone Black (BBB) and other components

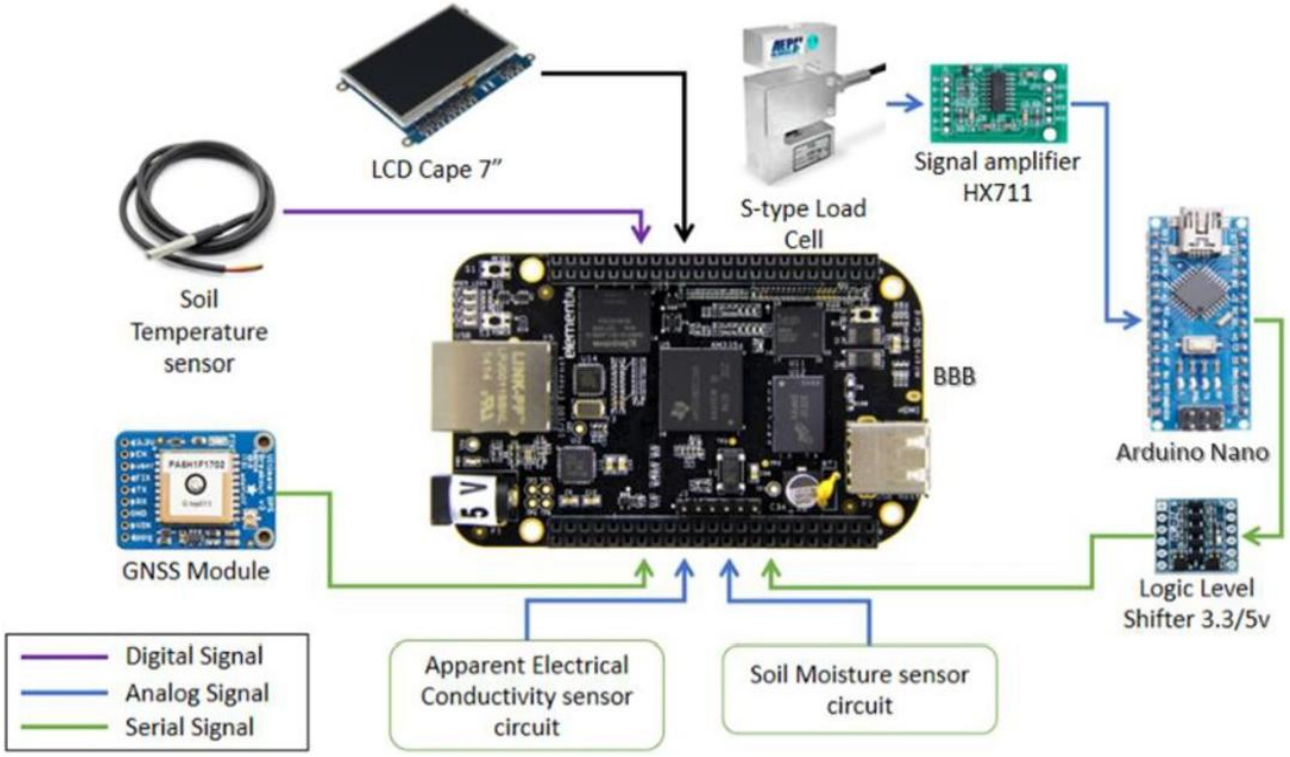


**Figure 2** - Circuit developed for soil moisture measurement, adapting the circuit for the astable operation mode of the 555 timer integrated circuit proposed by Texas Instruments (2014)

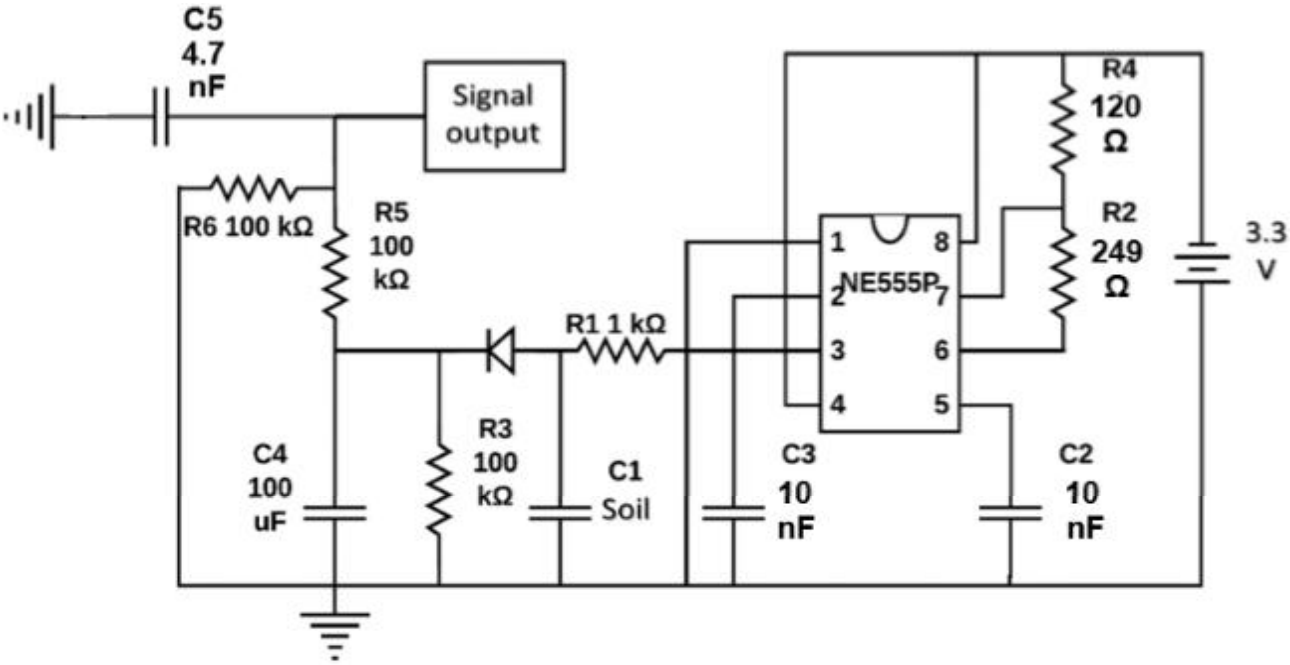

The DS18B20 sensor (Dallas Semiconductor, Texas, USA) was used to measure the soil temperature, with an operating range between -10 °C and 85 °C, an accuracy of 0.5 °C, and a 12-bit digital-to-analog converter. It contained a stainless-steel capsule with the diameter and length of 6 and 50 mm, respectively. The temperature sensor was fixed to an ECa sensor structure and connected to a digital BBB port.

The soil penetration resistance sensor comprises a penetration rod connected to a load cell. The penetration rod contained a conical tip and was constructed according to ASABE S313.3 standards (AMERICAN SOCIETY OF AGRICULTURAL AND BIOLOGICAL ENGINEERS, 2006). The rod had a diameter of 9.53 mm and a length of 400 mm, and the cone had the angle and diameter of 30° and 12.83 mm, respectively. The load cell used was a model for measuring tensile and compressive forces, with a maximum capacity of 1000 N (AEPH Brazil, Sao Paulo, Brazil). It was connected to an HX711 amplifier using a 24-bit digital-to-analog converter (Avia Semiconductor, China). An Arduino Nano and a 3.3/5-V bidirectional logic level converter were used to transfer the data from HX711 to the BBB. Communication between the Arduino Nano and BBB was implemented using a universal asynchronous receiver/transmitter communication protocol. In multisensor platform software, the force exerted during the rod's penetration into the soil was used to calculate the penetration resistance (expressed in kPa).

The load cell was calibrated in a hydraulic cylinder with a dynamometer ring capacity of 4000 N and deformation constant of 690 N $mm^{-1}$. Compression forces with magnitudes between 0 N and 966 N were applied to the load cell. The interval between measurements was 69 N, corresponding to a 0.1-mm deformation in the dynamometer ring. The force (product of the dynamometer ring deformation and deformation constant) and the value reported by HX711 were recorded in each measurement. Linear regression was conducted to determine the coefficients of the model that describes the force (in N) as a function of the value determined by HX711 (Figure 4).

The mechanical design of the multisensor platform was developed such that the device could be portable and its transport and operation could require only one operator. Rectangular aluminum tubing was used to build the structure of the ECa and moisture sensors. The structure of the ECa sensor was used to fix the central unit of the multisensor platform and to support moisture and penetration resistance sensors. Because soil moisture and ECa sensors operate by applying an electrical signal to the soil, the electrodes of both sensors were installed in two independent structures. Thus, simultaneous contact of the two sensors with the ground was prevented. A multi-sensor platform was developed for the use of one sensor at a time.

**Software developed for the multisensor platform**

The software for the soil multisensor platform was developed in C++ language using the integrated development environment Qt Creator 5.11.1 (Qt Company, Espoo, Finland). It was created using a graphical user interface comprising four screens (tabs): data file (Figure 5A), system settings (Figure 5B), workspace (Figure 5C), and maps (Figure 5D). The graphical user interface was displayed on a 178-mm LCD touchscreen connected to the BBB.

In the data file tab (Figure 5A), the implemented functions are creating, opening, and editing the data file. In the system settings tab (Figure 5B), the software allows the configuration of the operation and map generation parameters. The function implemented

**Figure 3** - Calibration curve of the soil moisture sensor used to obtain the moisture (in % dry base) as a function of the voltage value at the circuit output

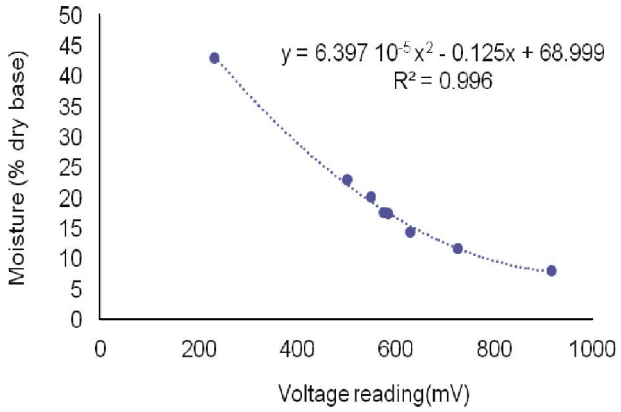


**Figure 4** - Calibration curve of the load cell used in the soil penetration resistance sensor to obtain the force (in N), depending on the value reported by the HX711 amplifier and analog-to-digital converter

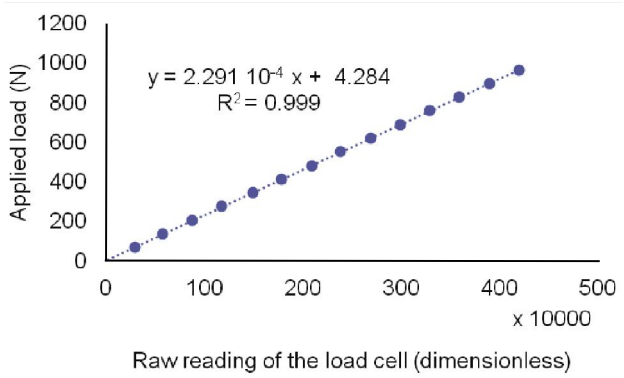

was the creation of a uniform sampling grid, with the distance between points defined by the user. To use this function, the user must first collect data on the contour of the area using the workspace tab (Figure 5C).

**Figure 5** - Screens of the multisensor platform software: (A) data file, (B) system settings, (C) workspace, and (D) show maps

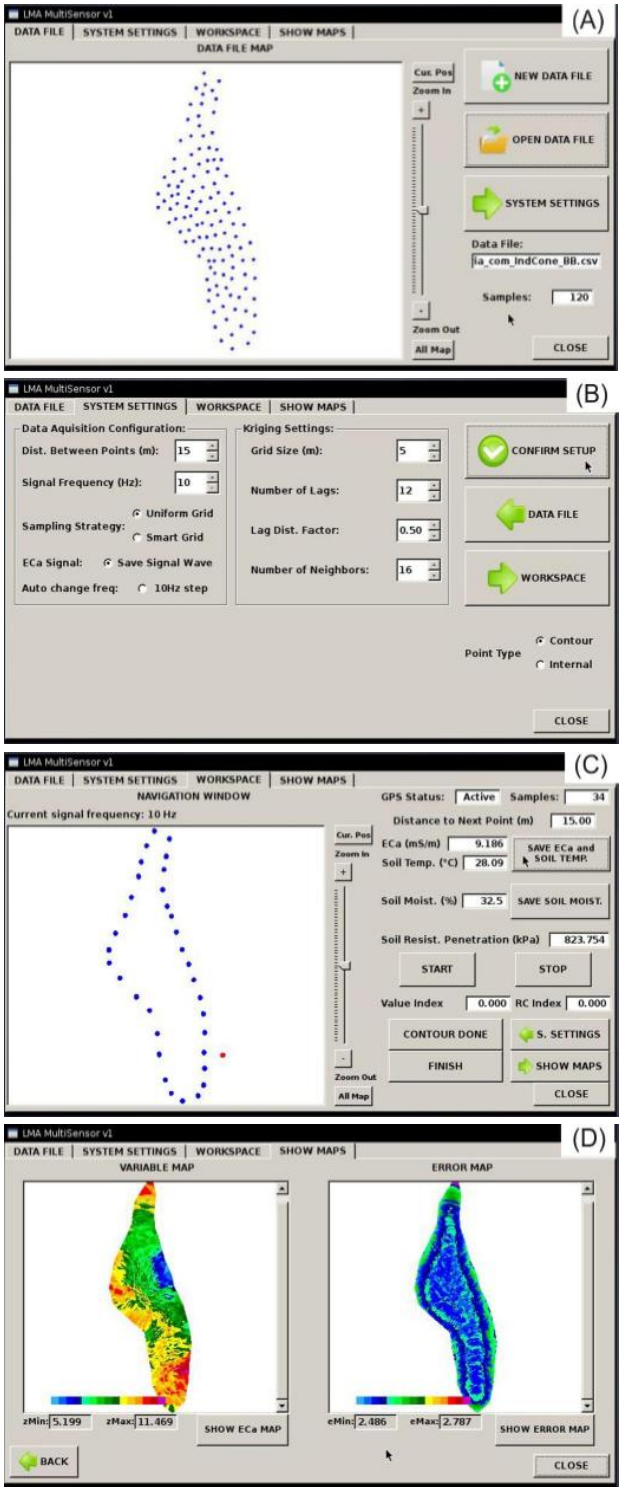


In the map tab (Figure 5D), geostatistical analysis of the collected data was conducted with the generation of an interpolated map by ordinary kriging (ISAAKS; SRIVASTAVA, 1989). To create the experimental semivariogram, the user can define the lag distance factor and the number of lags. The lag distance factor was used to calculate the active distance of the semivariogram from the maximum distance between sampled points. The semivariance in each lag was calculated using Equation (1):

$$\gamma = \frac{1}{2N}\sum_{i=1}^{N}(Z_{xi} - Z_{xi+h})^2 \quad (1)$$

where γ is the semivariance, N is the number of pairs of points for the lag, $Z_{xi}$ is the value of the variable at position i, and $Z_{xi+h}$ is the value of the variable at a distance h from position i. From the experimental semivariogram, the software fitted three models for the theoretical semivariogram: exponential, spherical, and Gaussian. The semivariogram parameters were fitted based on the minimization of the sum of the squared errors. The software used the lowest sum of squared errors to select the model to be adopted. The software generated a regular grid from the contour of the area to execute interpolation. The grid size is defined by the user. At each point of the grid, the software uses the values of the k nearest neighbors to calculate the estimated value (Equation 2).

$$Z^* = \sum_{i=1}^{k} w_i Z_i \quad (2)$$

where Z* is the estimated value, $w_i$ is the weight of neighbor i, and $Z_i$ is the value of the variable of neighbor i. The vector w, which contains the weights and Lagrangian multiplier, is obtained using Equation (3).

$$W = C^{-1}d \quad (3)$$

where $C^{-1}$ is the inverse of the estimated covariance matrix for each pair of observed values. Vector *d* is the estimated covariance vector between the observed and estimated values. Vector w comprises the weights of each neighbor and Lagrangian multiplier. Using this multiplier, the standard deviation of the estimated value at each point on the grid can be calculated (ISAAKS; SRIVASTAVA, 1989). The software showed the interpolation map and standard deviation map.

**Validation of the multisensor platform**

To validate the developed multisensor platform, ECa, soil moisture, and resistance to penetration were measured in an experimental area. The experimental area contained regions where the soil was conventionally prepared and regions of direct cultivation. In addition, there were both irrigated and non-irrigated crops. For each measurement point, variables were obtained using a multisensor platform and commercial sensors.

To measure soil ECa, a commercial portable sensor LandMapper ERM-2 (LandViser LLC, USA) was used, coupled to a structure with electrodes arranged in a line according to the Wenner matrix, spaced 30 cm apart. To measure soil moisture, a commercial FieldScout TDR300 sensor (Spectrum Technology, Inc., USA) with 12 cm electrodes. Data were collected at 30 sampling points to validate the ECa sensor and soil moisture of the multisensor platform.

To measure the penetration resistance, a commercial penetrometer (Falker, Brazil) was used with a shank with a 30° conical tip and a diameter of 12.83 mm. Nail insertion was performed manually at a speed close to 30 mm/s. The penetration resistance was measured in the soil layer from 0 to 0.4 m. Data were collected at 15 sampling points for the validation of the penetration resistance sensor. For each point of measurement of penetration resistance, the mean and maximum values were obtained. For each variable, Pearson's correlation coefficient was used to assess the correlation between the data collected using the commercial sensor and multisensor platform. Validation of the temperature sensor was not performed because its accuracy was provided by the manufacturer.

**Figure 6** - Distribution of the sampling points used in the field test of the multisensor platform

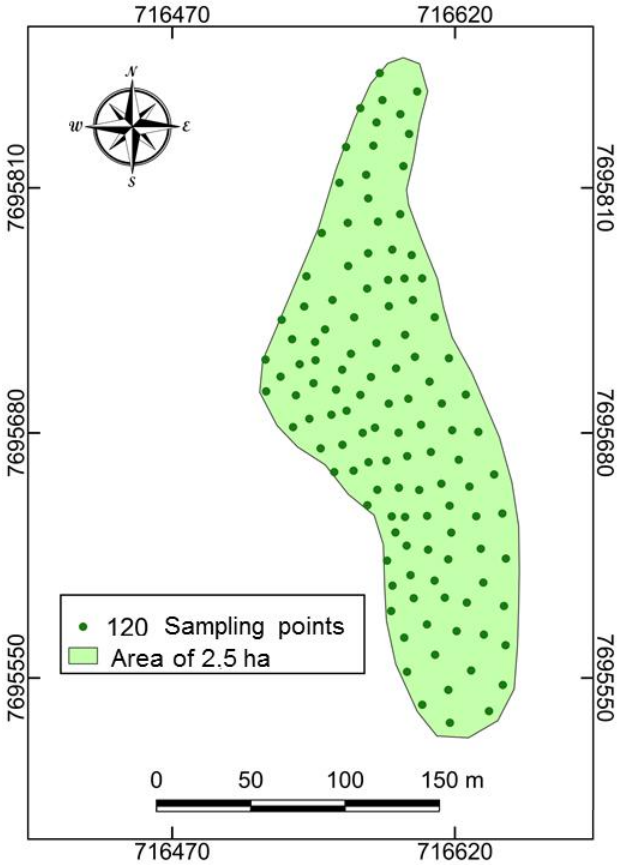


**Field test of the multisensor platform**

A multisensor platform was used to characterize the soil in an Arabica coffee plantation with an area of 2.5 ha, which was located in a region with predominantly clayey soil and a mountainous relief. Measurements were performed with soil close to field capacity. The four sensors were used for measurements at 120 points, with an average spacing of 14 m (Figure 6). For the soil ECa measurements, the adopted signal frequency was 10 Hz. The time taken for each measurement was recorded to determine the operational capacity of the multisensor platform.

**Validation of the map generation function**

The map-generating function was validated by comparing the maps from multisensor platform software with the maps generated by commercial software GS+ (Gamma Design Software, Michigan, USA) version 10. The penetration resistance variable was used for validation. For comparison, the interpolation grid and fitted semivariogram (model and parameters) obtained from multisensor platform software were used in GS+ software. The adopted grid size was 2.5 m. The interpolation and standard deviation maps generated by the two types of software (multisensor platform and GS+) were exported to QGIS software version 3.4.3 (QGIS Development Team, Open Source Geospatial Foundation, Chicago, IL, USA). The maps were compared by analyzing the range of the pixel values and distribution pattern of the pixel values.

**Analysis of the field test results**

Soil ECa, moisture, penetration resistance, and temperature data were transferred from the multisensor platform to a personal computer. After export, an analysis was performed to eliminate outliers. The outliers were those outside the range $\mu \pm 2.5\ \sigma$, where $\mu$ and $\sigma$ represent the mean and standard deviation of the data, respectively. In GS+ version 10, filtered data were used to generate a map interpolated by ordinary kriging. For the presentation of the maps, the data interpolated in GS+ were exported to QGIS.

## RESULTS AND DISCUSSION

The multi-sensor platform was built into modules (Figure 7). The cost of acquiring the components required to build the multisensor platform was US$ 361.94 (Table 1). This cost was achievable due to the use of open-source components, which have lower cost than closed-source components (FISHER; GOULD, 2012). To collect georeferenced data on ECa, soil moisture and penetration resistance using the three commercial sensors used in the validation, an investment of approximately US$ 2,500 was required, including a GNSS navigation receiver for

georeferencing the sample points. This investment was almost seven times greater than the cost of assembling the developed multisensor platform. The lower acquisition cost of the developed multisensor platform enables its use by smallholder farmers.

**Validation of the multisensor platform**

Soil ECa of the experimental area ranged from 1.0 to 17 m Sm-1 (Figure 8A). The soil moisture percentage in the experimental area is within 5–42% (Figure 8B). Note that the sensor of the multisensor platform was calibrated to present the gravimetric soil moisture, whereas the commercial Field Scout TDR sensor presented volumetric soil moisture. The average penetration resistance at depths of 0–0.4 m ranged from 500 to 2500 kPa (Figure 8C). The maximum penetration resistance at depths of 0–0.4 m ranged from 800 to 3700 kPa (Figure 8D).

**Figure 7** - Multisensor platform built in modules that allow disassembly for transport: (A) front view and (B) details of the moisture sensor (left). ECa sensor and temperature sensor (center) and penetration resistance sensor (right)

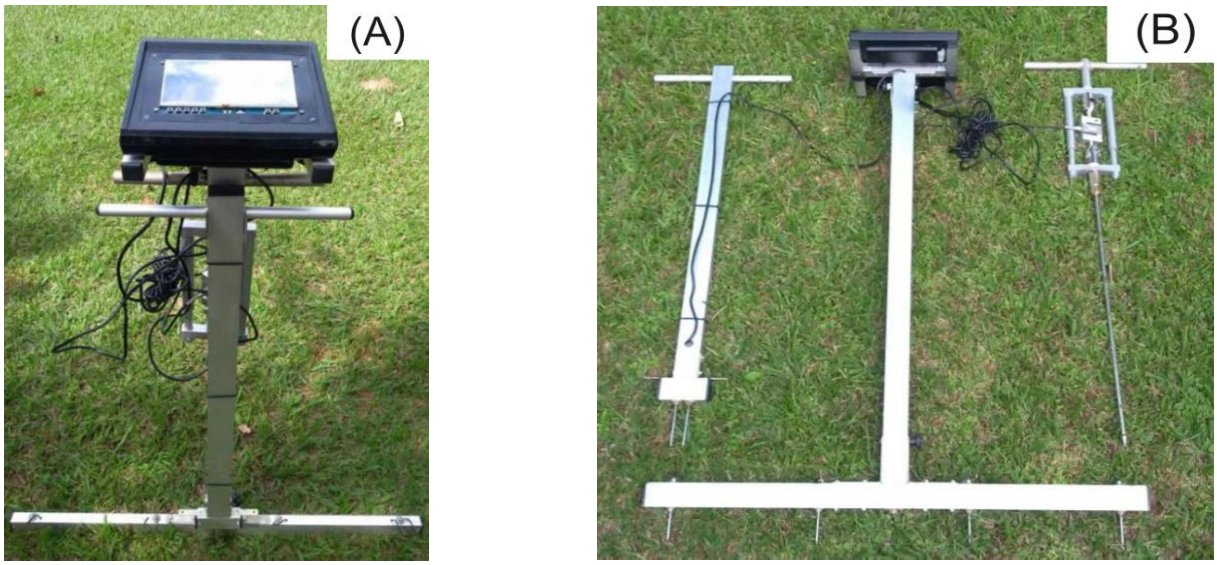


**Table 1** - Composition of the acquisition costs of the components used in the assembly of the multisensor platform

| Quantity | Description | Prices | |
|---|---|---|---|
| | | Unit* (US$) | Total (US$) |
| 1 | BeagleBone Black Rev.C | 61.00 | 61.00 |
| 1 | 4D Systems 178-mm LCD Cape touchscreen | 89.00 | 89.00 |
| 1 | Adafruit Ultimate GNSS module with 28-dBi external antenna | 47.00 | 47.00 |
| 1 | 16-Mhz 5-V Atmega 328P Arduino Nano | 4.00 | 4.00 |
| 1 | 3.3-5-V bidirectional logic converter | 1.50 | 1.50 |
| 1 | HX711 analog-to-digital converter amplifier | 1.50 | 1.50 |
| 1 | 1000-N load cell | 38.00 | 38.00 |
| 1 | 5-V 12000-mAh rechargeable battery | 15.95 | 15.95 |
| 1 | 50x25x2500-mm rectangular aluminum tubing | 39.99 | 39.99 |
| 1 | Steel tubing | 13.00 | 13.00 |
| 1 | Electrodes and screws in carbon steel | 20.0 | 20.00 |
| 1 | Plastic box | 11.00 | 11.00 |
| 1 | Various electronic components (e.g., wires, integrated circuits, resistors, capacitors, and connectors) | 20.00 | 20.00 |
| Total | 361.94 | | |

* Electronic components with prices obtained from Amazon and Mouser Electronics online stores on June 6, 2020

Pearson's correlation coefficients between the values of ECa, soil moisture, and mean and maximum penetration resistance measured with the multisensor platform and commercial sensors were 0.95, 0.92, 0.90, and 0.91, respectively. All correlation coefficients were significant at the 5% level by the t-test. Correlation coefficients with values close to one indicate a strong correlation between the data measured by the multisensor platform and the data measured by the commercial sensor. Therefore, the multisensor platform could provide data on soil variables with magnitudes and variability similar to those obtained with commercial sensors. The precision of the developed multisensor platform, associated with its low manufacturing cost, reinforces its potential for use, particularly for small-scale farmers.

The time required to perform the measurements of the ECa, moisture, temperature and penetration resistance at the coffee plantation with an area of 2.5 ha was approximately 7.0 h. Each variable was measured at 120 sampling points. This results in an average effective operational capacity of 17.14 sample points $h^{-1}$. The average times required to measure soil ECa, moisture, and penetration resistance were 2.0, 8.0, and 50 s, respectively. The soil temperature was measured simultaneously with the ECa measurement. Therefore, the theoretical operational capacity of the multisensor platform was 60 sample points $h^{-1}$ with an operational efficiency of 28.6%. The low operational capacity can be related to the time required for the operator to move between measuring points. Because it is a portable device and is not connected to a vehicle, the multisensor platform can be used in areas inaccessible by wheeled vehicles (e.g., on terrains with steep slopes and in small areas).

**Validation of the map generation function**

In multisensor platform software, the model selected in the theoretical semivariogram was Gaussian. The values of the nugget effect, range, and sill parameter were 17,344.42 $kPa^2$, 63.44 m, and 27093.16 $kPa^2$, respectively. The same model and parameters of the theoretical semivariogram were adopted in GS+ software. Comparison of the interpolation maps of soil penetration resistance indicates the similarities in the pixel values calculated using both types of software (Figures 9A and 9B). In the interpolation map generated by GS+ software, the pixel values varied from 491 to 796 kPa. In the map generated by the multisensor platform, the pixel values varied from 511 kPa to 784 kPa. The same distribution pattern of pixel values was observed in maps generated by both software types. That is, the minimum and maximum value classes occurred in the same region on both maps. Therefore,

**Figure 8** - Multisensor platform validation with commercial sensors: (A) soil ECa data collected with the multisensor platform and LandMapper ERM-02. (B) Soil moisture data collected with the multisensor platform and FieldScout TDR 300. (C) and (D) Soil penetration resistance, mean, and maximumdata collected with the multisensor platform and Falker PLG1020

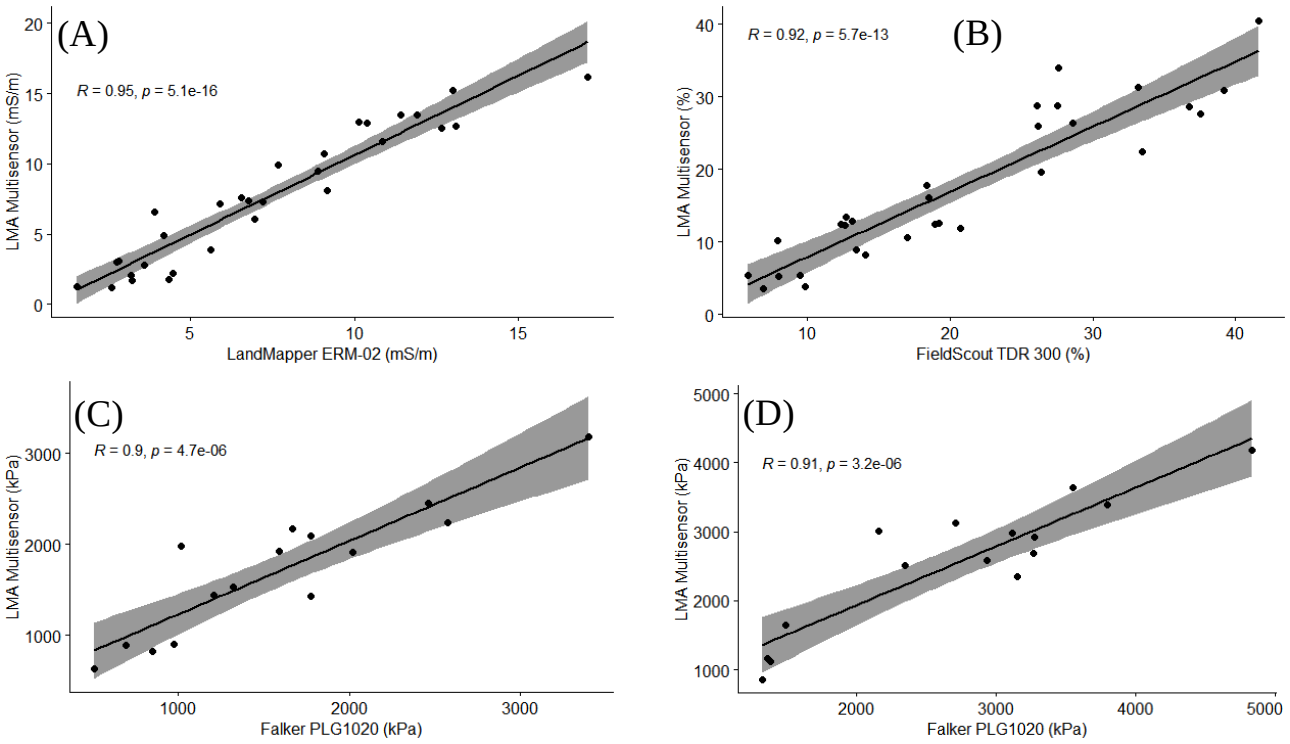

the map generation function developed for the multisensor platform can be used to analyze the spatial variability of the variables measured by the sensors.

For the standard deviation map, the pixel values varied from 147 to 161 kPa and 137 to 148 kPa in the maps generated by GS+ and the multisensor platform, respectively (Figures 9C and 9D). Based on the spatial distribution of the sampling points (Figure 6), this behavior occurred because of the lower density of the points in this region. Kumar and Remadevi (2006) observed the influence of the quantity and location of the sampling points on the standard deviation map. Lower standard deviations were also observed in regions with higher sampling densities.

**Figure 9** - Interpolated map of the penetration resistance generated by the software (A) GS+ and (B) that of the multisensor platform and standard deviation map generated by software (C) GS+ and (D) that of the multisensor platform

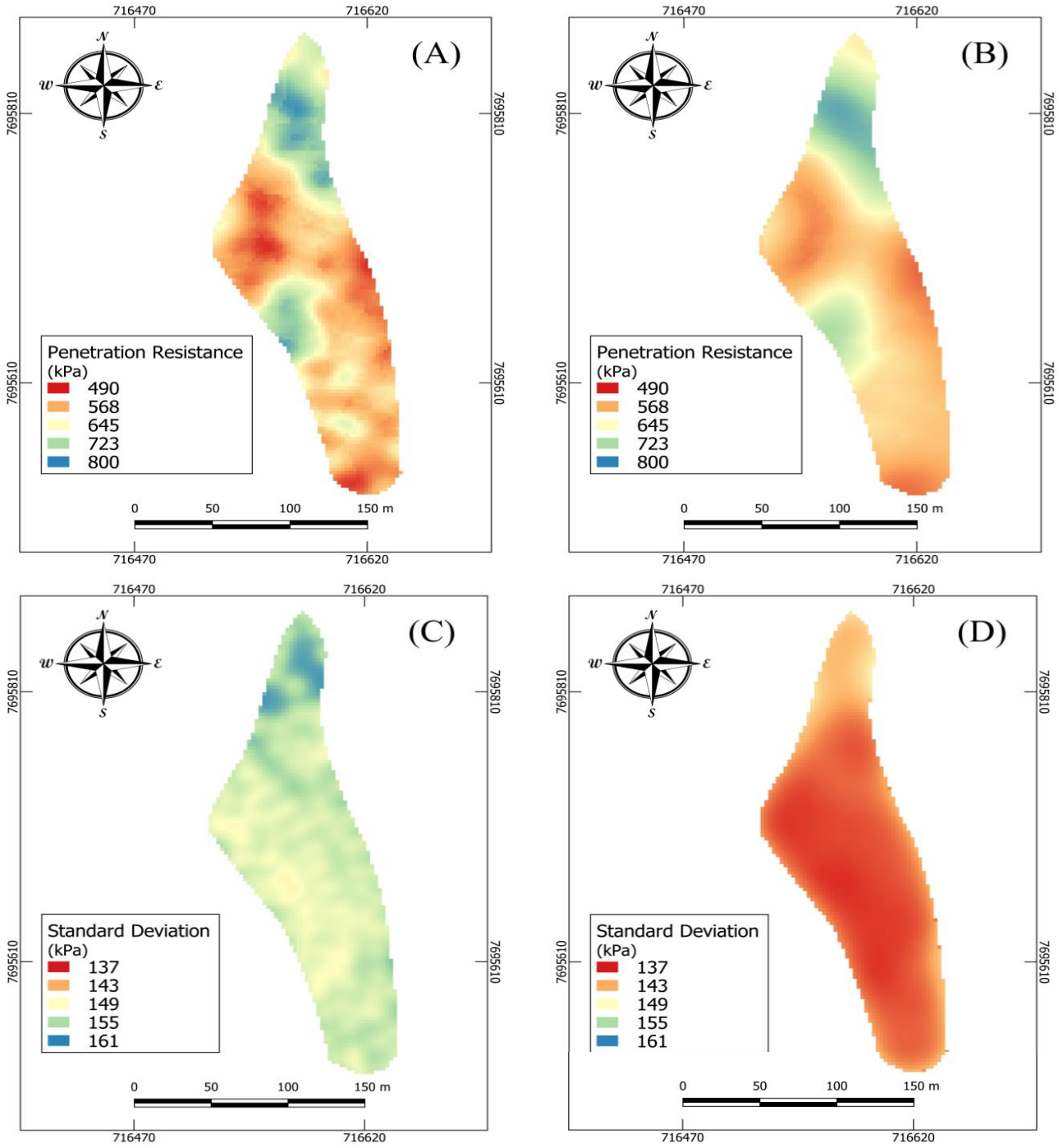

**Analysis of the field test results**

The analysis performed to remove outliers resulted in the removal of four (3.3%), four (3.3%), zero (0%), and five (4.2%) points for ECa, moisture, temperature, and penetration resistance, respectively. In GS+ software, the semivariogram models fitted to the filtered data were exponential and spherical for the ECa and other variables, respectively (Table 2). For the four variables, the range parameter was greater than the mean distance between sampled points (approximately 14 m). Therefore, the adopted sampling density was sufficient to detect the spatial dependence of the studied variables (AYOUBI; MOHAMMAD ZAMANI; KHORMALI, 2007).

The spatial distributions of the soil ECa and moisture were similar (Figures 10A and 10B). Therefore, these variables show a positive correlation (MOLIN; FAULIN, 2013; SUDDUTH *et al*., 2005). The northern and southern regions had lower soil temperatures (Figure 10C) caused by the shade cast by trees. As the temperature variation was less than 10 °C, the ECa need not be adjusted to the reference temperature of 25 °C (CORWIN; LESCH, 2005).

The penetration resistance map (Figure 10D) does not show any correlation with the maps obtained for the other variables. In this case, the spatial distribution of this variable can be more related to

**Table 2** - Theoretical semivariance parameters adjusted using GS+ software for experimental data obtained with the developed multisensor platform after outlier removal

| Variable | Model | Range (m) | $R^2$ | SSR** |
|---|---|---|---|---|
| ECa* | exponential | 154.8 | 0.94 | 0.85 $mS^2.m^{-2}$ |
| Moisture | spherical | 38.2 | 0.72 | 10.20%$^2$ |
| Temperature | spherical | 89.4 | 0.96 | 0.06 $ºC^2$ |
| Penetration resistance | spherical | 129.7 | 0.96 | 1.30 107 $kPa^2$ |

* Soil apparent electrical conductivity; ** Sum of squared residuals

**Figure 10** - Maps of the (A) apparent soil electrical conductivity (ECa) at 10 Hz, (B) moisture, (C) temperature, and (D) penetration resistance variables generated using software GS+ for data obtained with the developed multisensor platform after outlier removal

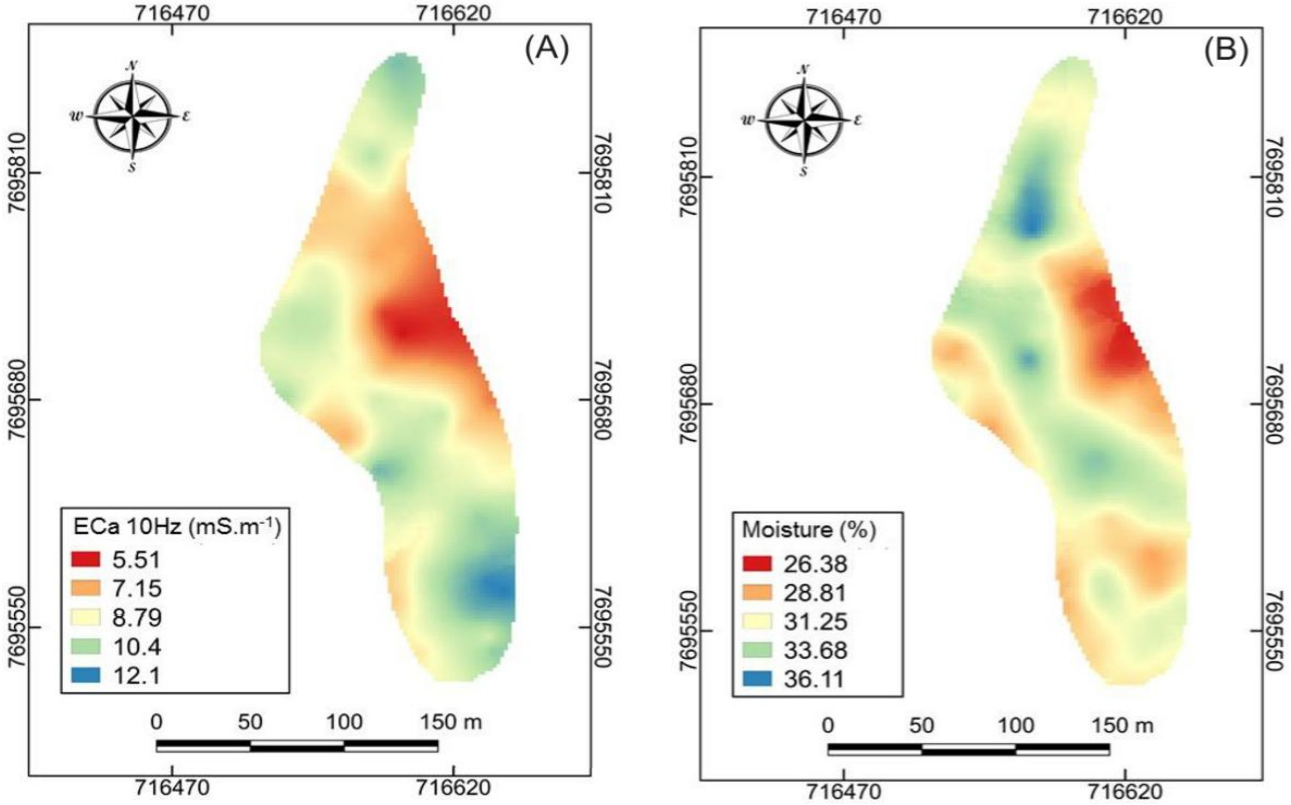

*Continuation Figure 10*

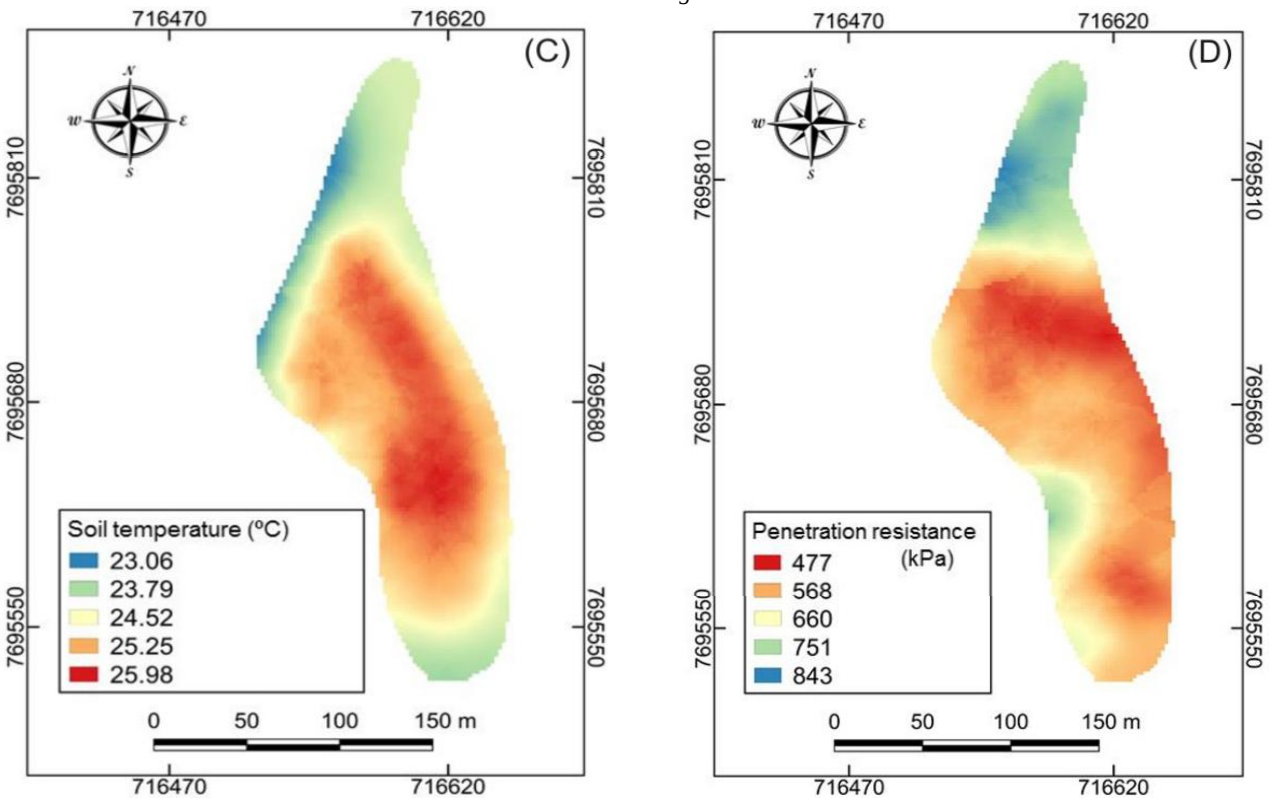


clay content, organic matter content, and soil physical properties (CHEN *et al*., 2012; CHO; SUDDUTH; CHUNG, 2016). By comparing the maps generated with the raw (Figure 8A) and filtered (Figure 9D) data, the similarity of the distribution patterns of the pixel values was observed. However, the penetration resistance at each point has a change, which can be attributed to the models and parameters of the semivariogram used in each case.

## CONCLUSIONS

The cost of acquisition of the components needed to assemble the multisensor platform was US$ 361.94. The correlation obtained in the comparison between the data obtained with the multisensor platform and commercial sensors was high and significant. The map generation function resulted in maps similar to those generated by commercial software for the same analysis. The standard deviation map enabled the evaluation of the quality of the spatial distribution of the sampling points. The spatial variability of ECa, moisture, temperature, and penetration resistance in a coffee plantation were analyzed using the maps generated with the data obtained by the four sensors.

## ACKNOWLEDGMENTS

We acknowledge the National Council for Research and Development (CNPq) and the Coordination for the Improvement of Higher Education Personnel (CAPES - Funding Code 001) for their financial support for this study and Editage (www.editage.com) for English language editing.

## REFERENCES

ADAMCHUK, V. I. *et al*. On-the-go soil sensors for precision agriculture. **Computer and Electronics in Agriculture**, v. 44, n. 1, p. 71-91, 2004.

AMERICAN SOCIETY OF AGRICULTURAL AND BIOLOGICAL ENGINEERS. Soil cone penetrometer. Saint Joseph, 2006. p. 902-904. (ASABE standard: ASAE S313.3 FEB04).

AYOUBI, S.; MOHAMMAD ZAMANI, S.; KHORMALI, F. Spatial variability of some soil properties for site specific farming in northern Iran. **International Journal of Plant Production**, v. 1, n. 2, p. 225-236, 2007.

CHEN, Y. *et al*. Soil penetration resistance in relation to soil texture, moisture content, and bulk density for no-tillage and conventional tillage. **Agriculture Engineering International: CIGR Journal**, v. 14, n. 1, p. 26-37, 2012.

CHO, Y.; SUDDUTH, K. A.; CHUNG, S.-O. Soil physical property estimation from soil strength and apparent electrical conductivity sensor data. **Biosystems Engineering**, v. 152, n. 1, p. 68-78, 2016.

COELHO, A. L. F. *et al*. Development of a variable-rate controller for a low-cost precision planter. **Applied Engineering in Agriculture**, v. 36, n. 2, p. 233-243, 2020.

CORWIN, D. L.; LESCH, S. M. Apparent soil electrical conductivity measurements in agriculture. **Computer and Electronics in Agriculture**, v. 46, n. 1/3, p. 11-43, 2005.

FISHER, D. K.; GOULD, P. J. Open-source hardware is a low-cost alternative for scientific instrumentation and research. **Modern Instrumentation**, v. 1, n. 2, p. 8-20, 2012.

FISHER, D. K.; KEBEDE, H. A low-cost microcontroller-based system to monitor crop temperature and water status. **Computer and Electronics in Agriculture**, v. 74, n. 1, p. 168-173, 2010.

ISAAKS, E. H.; SRIVASTAVA, R. M. An introduction to applied geostatistics. New York: Oxford University Press, 1989. 561 p.

KUMAR, V.; REMADEVI, P. Kriging of groundwater levels: a case study. **Journal of Spatial Hydrology**, v. 6, n. 1, p. 1-12, 2006.

MAHMOOD, H. S.; HOOGMOED, W. B.; VAN HENTEN, E. J. Sensor data fusion to predict multiple soil properties. **Precision Agriculture**, v. 13, n. 1, p. 628-645, 2012.

MEDEIROS, W. N. *et al*. The temporal stability of the variability in apparent soil electrical conductivity. **Bioscience Journal**, v. 32, n. 1, p. 150-159, 2016.

MOLIN, J. P.; FAULIN, G. D. C. Spatial and temporal variability of soil electrical conductivity related to soil moisture. **Scientia Agricola**, v. 70, n. 1, p. 1-5, 2013.

MOLLOY, D. Exploring BeagleBone: tools and techniques for building with embedded Linux. Indianapolis: John Wiley & Sons, 2014. 600 p.

NADERI-BOLDAJI, M. *et al*. A mechanical-dielectric-high frequency acoustic sensor fusion for soil physical characterization. **Computers and Electronics in Agriculture**, v. 156, n. 1, p. 10-23, 2019.

QUEIROZ, D. M. *et al*. Development and testing of a low-cost portable apparent soil electrical conductivity sensor using a Beaglebone Black. *In*: **2017 ASABE Annual International Meeting**. St. Joseph: ASABE, 2017. (Paper Number 1700062).

QUEIROZ, D. M. *et al*. Development and testing of a low-cost portable apparent soil electrical conductivity sensor using a Beaglebone Black. **Applied Engineering in Agriculture**, v. 36, n. 3, p. 341-355, 2020.

QUEIROZ, D. M.; LEE, W. S.; SCHUELLER, J. K. Development of a portable soil sensor system using BeagleBone Black. *In*: **2016 ASABE Annual International Meeting**. St. Joseph: ASABE, 2016. (Paper Number 162447581).

STADLER, A. *et al*. Quantifying the effects of soil variability on crop growth using apparent soil electrical conductivity measurements. **European Journal of Agronomy**, v. 64, n. 1, p. 8-20, 2015.

SUDDUTH, K. A. *et al*. Relating apparent electrical conductivity to soil properties across the north-central USA. **Computer and Electronics in Agriculture**, v. 46, n. 1/3, p. 263-283, 2005.

TEIXEIRA, P. C. *et al*. Manual de métodos de análise de solo. 3. ed. Brasília: Embrapa Solos, 2017. 573 p.

TEXAS INSTRUMENTS. Precision Timers NA555, NE555, SA555, SE555 datasheet. Dallas: Texas Instruments, 2014. 37 p.

YURUI, S. *et al*. Determining soil physical properties by multi-sensor technique. **Sensors and Actuators A: Physical**, v. 147, n. 1, p. 352-357, 2008.